Computer Models for Optimizing Interventions in Refractory Pulmonary Hypertension

Seong Woo Han BS[1], Charles Puelz PhD[2], Craig G. Rusin PhD[2],
Dan J. Penny MD, PhD, MHA[2], Ryan Coleman MD[2], and Charles S. Peskin PhD[1]

[1]Courant Institute of Mathematical Sciences, New York University
[2]Department of Pediatrics-Cardiology, Baylor College of Medicine

January 1, 2021

Abstract

This paper describes computer models for three surgeries used in treating refractory pulmonary hypertension. These treatments create (1) an atrial septal defect (ASD), (2) a ventricular septal defect (VSD), or (3) a patent ductus arteriosus (PDA). The aim in all three cases is to generate a right-to-left shunt that allows blood partially to bypass the lungs, thereby lowering the pulmonary artery pressure. This lower pressure requires introducing de-oxygenated blood into the systemic circulation, thereby lowering the systemic arterial oxygen saturation. The models in this paper are based on compartmental descriptions of human hemodynamics and oxygen transport. An important parameter in our models is the cross-sectional area of the surgically created defect. Numerical simulations are performed to compare the different interventions and to assess the effect of the defect on the hemodynamic variables and oxygen saturations in each of the three surgically modified circulatory systems.

1   Introduction

Pulmonary hypertension refers to a spectrum of cardiovascular disease that involves elevated blood pressure in the pulmonary arterial circulation. In this paper, our focus is on refractory pulmonary hypertension, which corresponds to disease that is unresponsive to standard medical treatments [4, 7]. In this case, more extreme measures are taken, including catheter-based interventions, to off-load extremely high pressures on the right side of the heart [6]. The focus of this paper is on three possible surgical interventions that create connections not normally present in a healthy circulation.

The three surgically created connections that we consider are either within the (1) atrial septum, (2) ventricular septum, or (3) between the main pulmonary artery and aorta [6, 2]. We refer to these surgically created defects by names that are commonly used for the congenital heart disease states in which they occur naturally. They are (1) an atrial septal defect (ASD), (2) a ventricular septal defect (VSD), and (3) a patent ductus arteriosus (PDA). In all cases, the goal is to create a right-to-left shunt that allows a portion of blood to bypass the lungs, potentially lowering the pulmonary artery pressure. While each of these three interventions potentially creates the required shunt, their performance is not clear within the context of a beating heart that generates complicated pressure dynamics. Further, their performance is highly sensative to shunt size, a variable that can easily be varied within the computational models described in this paper.

1

Blood that bypasses the lungs is not fully oxygenated, so an important potential downside of such an intervention is a lowering of the systemic arterial oxygen saturation. For each intervention, we develop and apply computational models to study both the benefit in terms of reduced pulmonary artery pressure and also the detriment in terms of systemic arterial oxygen desaturation, as functions of the cross-sectional area of the shunt created by the surgeon.

Pulmonary hypertension is a challenging disease with several classes and multiple treatment options, some of which are still experimental. These complexities have motivated the use of computational models for "non-invasively" studying disease progression, diagnosis, and the performance of different treatments. We recall several physics-based models of the human circulation with pulmonary hypertension that exist in the literature. Delhass et al. constructed compartment models for two possible interventions considered in this paper, the ASD and the PDA [3]. These authors referred to the latter intervention as the Potts shunt. Our paper extends their results to a comparison of the ASD and PDA with the VSD. Acosta et al. used vessel network models of pulmonary hypertension to derive early diagnostic indicators of disease [1]. Qureshi et al. developed structured-tree models coupled to vessel network models of the arterial and venous circulations to computationally study several classes of pulmonary hypertension [11].

2   Circulation Models and Numerical Methods

In this section, we describe the models used in this work and the numerical methods by which the model equations are solved. The following subsections discuss a hemodynamic model, a cardiac chamber model that specifies the time-varying compliance of each heart chamber in the hemodynamic model, a shunt model based on the Gorlin equation that makes it possible to include shunts of specified cross-sectional area in the hemodynamic model, and finally an oxygen transport model that calculates oxygen saturations throughout the model circulation based on the flows obtained from the hemodynamic model.

2.1   Hemodynamic model

The circulation is represented by a collection of compartments corresponding to compliance chambers connected by resistors that are equipped with valves [10]. We use the following compliance relation for each of the N compliance chambers, numbered $i = 1, 2, ..., N$

$$V_i = (V_d)_i + C_i P_i, \quad i = 1, ..., N, \tag{1}$$

The parameter C_i is the compliance of chamber i, which is assumed to be constant for arteries and veins but time-varying for the heart chambers. The variable V_i is the volume of compliance chamber i, the variable P_i is the pressure of that chamber, and the parameter $(V_d)_i$ is the dead volume, that is, the volume of the chamber when the pressure is zero.

We assume that the flow from chamber i to chamber j is governed by a pressure-flow relationship of the following form:

$$Q_{ij} = \frac{S_{ij}}{R_{ij}}(P_i - P_j) = S_{ij}\, G_{ij}\, (P_i - P_j), \quad i, j = 1, ..., N, \tag{2}$$

where

$$S_{ij} = \begin{cases} 1, & P_i > P_j, \\ 0, & P_i \le P_j. \end{cases} \tag{3}$$

Equation (2) describes the flow through a resistance that is equipped with a valve. The conductance G_{ij} is the reciprocal of the resistance R_{ij}. Conductance is convenient because it can be set equal to zero to represent the absence of a connection. The variable S_{ij}, which is determined by P_i and P_j according to equation (3), denotes the state of the valve, with $S_{ij} = 1$ when the valve is open, and $S_{ij} = 0$ when the valve is closed. (Note that the words "open" and "closed" have the opposite meaning here from their use in electricity, where a closed switch is conducting and an open switch is non-conducting.)

Equipping *every* connection with a valve does not involve any loss of generality. Between any pair of chambers i and j, our framework allows for *two* connections of the type described above, one with a valve that allows flow only from i to j, and another with a valve that allows flow only from j to i. To model a situation in which there is no valve in a connection between chambers i and j, we need only set G_{ij} equal to G_{ji}. To model a leaky valve we may set G_{ij} and G_{ji} to positive but unequal values. Lastly, to model the situation in which there is no connection at all between chambers i and j, we set $G_{ij} = G_{ji} = 0$. Thus, our framework allows us to model a great variety of connection types and patterns merely by specifying the (non-symmetric) N by N matrix G.

We differentiate equation (1) with respect to time and use the principle that the rate of change of volume is equal to inflow minus outflow, together with equation (2), to obtain the following system of ordinary differential equations for the pressures as functions of time.

$$
\begin{aligned}
\frac{d}{dt}(C_i P_i) &= \sum_{j=1}^{N}(S_{ji}G_{ji}(P_j - P_i) - S_{ij}G_{ij}(P_i - P_j)) \\
&= \sum_{j=1}^{N}(S_{ij}G_{ij} + S_{ji}G_{ji})(P_j - P_i).
\end{aligned} \tag{4}
$$

We have assumed here that all of the dead volumes are constant, but we have allowed for the possibility that some of the compliances, specifically those of the heart chambers, are functions of time. How these compliances are specified will be described in section 2.2. Equation (4) will be modified later to include shunt flows modeled by the Gorlin equation, see section 2.3.

Our numerical scheme for equation (4) is the backward-Euler method:

$$
\frac{C_i^n P_i^n - C_i^{n-1} P_i^{n-1}}{\Delta t} = \sum_{j=1}^{N}(S_{ij}^n G_{ij}^n + S_{ji}^n G_{ji}^n)(P_j^n - P_i^n). \tag{5}
$$

This is a system of equations for the unknown pressures at time step n. It is a nonlinear system, because S_{ij} is a function of P_i and P_j, see equation (3). The reason for using the backward-Euler method here is its unconditional stability. If two compliance chambers are connected by a very large conductance (that is, by a very small resistance), their pressures will equilibrate on a very fast time scale, and we do not want to be required to use a small enough time step to resolve the details of that rapid equilibration. This situation actually arises in the circulation whenever there are two chambers with an open heart valve between them, since an open heart valve (at least when it is non-stenotic) has a very high conductance.

The procedure that we use to solve the nonlinear system (5) is based on the following observation: given the valve states, equation (5) is a linear system that is easy to solve for the pressures. Also, given the pressures, it is easy to evaluate the valve states from equation (3). Thus, the procedure starts with a guess for the valve states (a good guess is the valve states that were found on the

Parameters	Resistance (R)	Dead Volume (V_d)	Compliance (C)	Blood Volume (V)
Units	mmHg/(L/min)	L	L/mmHg	L
S	17.5	-	-	-
P	26.25	-	-	-
Mi	0.01	-	-	-
Ao	0.01	-	-	-
Tr	0.01	-	-	-
Pu	0.01	-	-	-
SA	-	0.825	0.00175	-
PA	-	0.0382	0.00175	-
SV	-	0	1.75	-
PV	-	0	0.08	-
V_{total}	-	-	-	8.68

Table 1: Parameters of the Model Circulation: Pulmonary resistance is chosen very high, 1.5 times greater than the systemic resistance, to simulate refractory pulmonary hypertension. Abbreviations: S, systemic; P, pulmonary; Mi, mitral valve; Ao, aortic valve; Tr, tricuspid valve; Pu, pulmonic valve; SA, systemic artery; PA, pulmonary artery; SV, systemic vein; PV, pulmonary vein; V_{total}, total blood volume.

previous time step), solves equation (5) for the pressures, resets the valve states according to the pressures via equation (3), and so on. The process stops when the valve states (and therefore the pressures) stop changing, and in practice this happens very quickly. On most time steps, the initial guess, that the valves states are the same as they were at the previous time step, turns out to be correct. Also, when the valve states stop changing, the problem stated in equation (5) is actually solved (except, of course, for round-off error), not merely solved to within some tolerance. This is because the valve states are discrete.

For further discussion of the methodology described here, see [5]. As in that reference, we use six compliance chambers corresponding to the left and right ventricles and the systemic and pulmonary arteries and veins. We do not separately model the atria, but instead treat each atrium as part of the venous system to which it is connected, and moreover we do not take into account the time dependence of the atrial compliances. The ventricular compliances are, of course, time dependent in our model, but not in the same way as in [5], see section 2.2.

In order to model pulmonary hypertension, we have made the pulmonary resistance 1.5 times greater than the systemic resistance. This is very different from the normal case in which the pulmonary resistance is about 6 times *smaller* than the systemic resistance. A consequence of pulmonary hypertension is right-heart hypertrophy, making the normally thin-walled right ventricle into a chamber that more closely resembles the normal left ventricle. To model this, we use typical left-ventricular parameters for both ventricles; see the next section. Another consequence of refractory pulmonary hypertension is right heart failure which leads to increased blood volume. Accordingly, we use a total blood volume of 8.68 L, instead of a normal blood volume, which would be about 5 L. This change is needed to elevate the systemic venous pressure sufficiently to fill the hypertrophied right heart and produce a viable cardiac output. With these exceptions, we are using the same parameters as in [5]. The non-cardiac hemodynamic parameters used in the present model are stated in Table 1.

2.2 Cardiac chamber model

In this section, we describe the time-varying elastance model used for the left and right ventricles, adapted from [9]. Note that the elastance, denoted by E, is the reciprocal of the compliance C. For a cardiac chamber, the elastance, and therefore the compliance, is a given function of time. In this work, we use the same elastance function $E(t)$, with the same parameters, for the left and right ventricles. This is because we are modeling pulmonary hypertension, in which the right ventricular wall thickens and becomes more like that of the left ventricle. The maximum and minimum ventricular elastances are denoted $E_{\max}$ and $E_{\min}$. E_{max} is the end-systolic elastance and E_{min} is the end-diastolic elastance. The functional form of the elastance $E(t)$ is given during the time interval $[0, T]$ as follows:

$$E(t) = k \left(\frac{g_1(t)}{1 + g_1(t)} \right) \left(\frac{1}{1 + g_2(t)} - \frac{1}{1 + g_2(T)} \right) + E_{min}, \tag{6}$$

where

$$g_1(t) = \left(\frac{t}{\tau_1} \right)^{m_1}, \quad g_2(t) = \left(\frac{t}{\tau_2} \right)^{m_2} \tag{7}$$

Here T is the period of the heartbeat. Note that equation (6) makes $E(0) = E(T)$. (We have made a slight modification of the formula used in [9] to ensure this.) Outside of the interval $[0, T]$, we define $E(t)$ as a periodic function with period T, so that $E(t) = E(t+T)$ for all t. The parameter k is chosen so that the maximum value of $E(t)$ is $E_{\max}$. The formula for k to achieve this is

$$k = \frac{E_{\max} - E_{\min}}{\max_{t \in [0,T]} [(\frac{g_1(t)}{1+g_1(t)})(\frac{1}{1+g_2(t)} - \frac{1}{1+g_2(T)})]} \tag{8}$$

The maximum in the denominator of the formula for k is computed by evaluating the expression that needs to be maximized at a collection of equally spaced points within the interval $[0, T]$, and then choosing the largest of the values of that expression that are found. Although this procedure does not yield the exact maximum value, it comes close enough for practical purposes, especially since the goal is to find the maximum value, rather than the time at which it occurs. Note that the evaluation of k only has to be done once for any particular choice of the parameters τ_1, m_1, τ_2, m_2, and T. Parameter values used for the heart chambers are provided in Table 2. The constant τ_1 controls the timescale of contraction, τ_2 controls the duration of systole, and m_1 and m_2 govern the speed of contraction and relaxation respectively. Note that τ and m are estimated from previously employed values [13], and the values for $E_{\min}$ and $E_{\max}$ are similar to those used by [8]. We have taken these parameters for a healthy left heart and applied them on both sides of the heart.

2.3 Shunt model

The Gorlin equation is used to calculate flows through surgically created shunts (ASD, VSD, or PDA) in our model [12]. This allows us to specify the cross-sectional area of the connection that the surgeon creates, and to study how area of the shunt affects the state of the circulation.

Consider two chambers, denoted by the indices 1 and 2, separated by a wall with a hole in it, and let A_0 be the cross-sectional area of the hole. We assume that the velocity of the blood as it goes through the hole is so much larger than the velocity in the two chambers that we may consider the fluid in each of the two chambers as if it were at rest. Let Q be the volume of blood flow per unit time through the hole, with the direction from chamber 1 to chamber 2 considered positive. Then the spatially averaged velocity of blood flow in the hole itself is given by

Parameters	Symbol	Units	Left Ventricle	Right Ventricle
Minimal elastance	$E_{\min}$	mmHg/L	0.08×1000	0.08×1000
Maximal elastance	$E_{\max}$	mmHg/L	30.00×1000	30.00×1000
Contraction exponent	m_1	-	1.32	1.32
Relaxation exponent	m_2	-	27.4	27.4
Systolic time constant	τ_1	min	0.269T	0.269T
Diastolic time constant	τ_2	min	0.452T	0.452T
Dead Volume	V_d	L	0.010	0.010
Period of heartbeat	T	min	0.0125	0.0125

Table 2: Parameters of the Heart Model.

$$v = Q/A_0. \tag{9}$$

Let P_1 and P_2 be the pressures in the two chambers, and let P_0 be the pressure within the hole. Suppose, for example, that $Q > 0$. By Bernoulli's equation in the upstream chamber up to the hole itself,

$$P_0 = P_1 - \frac{1}{2}\rho v^2 \tag{10}$$

$$= P_1 - \frac{\rho}{2A_0^2}Q^2. \tag{11}$$

In the region downstream of the hole, Bernoulli's equation does not apply because the flow there is dominated by turbulent eddies that dissipate energy. The result is that the pressure is relatively constant in the downstream region:

$$P_2 = P_0. \tag{12}$$

It follows that

$$P_1 - P_2 = \frac{\rho}{2A_0^2}Q^2, \quad Q > 0. \tag{13}$$

By the same reasoning, for flow in the other direction

$$P_2 - P_1 = \frac{\rho}{2A_0^2}Q^2, \quad Q < 0. \tag{14}$$

Equations (13) and (14) can be combined as follows:

$$P_1 - P_2 = \frac{\rho}{2A_0^2}|Q|Q, \tag{15}$$

and this shows that the hydraulic resistance of the hole is given by

$$R_{\text{shunt}} = \frac{\rho}{2A_0^2}|Q|. \tag{16}$$

Note that the above formula for R_{shunt} is independent of viscosity. In reality, there is a very small viscous resistance as well, so we modify the above formula to read

$$R_{\text{shunt}} = R_{\text{visc}} + \frac{\rho}{2A_0^2}|Q|. \tag{17}$$

In most situations R_{visc} is negligible, but we should include it to prevent R_{shunt} from being zero, which would otherwise happen in principle every time that Q changes sign. Since R_{visc} is included only for this reason, we choose the very small value $R_{\text{visc}} = 0.1\ mmHg/(liter/min)$. Evaluating the conductance of the hole from equation (17), we get

$$G_{\text{shunt}} = \frac{1}{R_{\text{visc}} + \frac{\rho}{2A_0^2}|Q|} \tag{18}$$

In making use of equation (18), we have to be careful about units. In this paper, we use what may be called physiological units, in which volume is measured in liters, pressure in $mmHg$, and time in minutes. The constants A_0 and ρ need to be expressed in these units. The use of liters for volume implies that our unit of length is the decimeter (dm), which is equal to 10 cm. Thus, A_0 needs to be expressed internally in terms of dm^2, although we convert on input and output to cm^2 since those units will have more meaning to the reader. To express density in physiological units, we need the units of mass. The units of force are $mmHg \cdot dm^2$, and the units of acceleration are dm/min^2, so the units of mass are $mmHg \cdot dm \cdot min^2$. Dividing this by dm^3, we get the units of density as $mmHg \cdot (min/dm)^2$. Note that

$$1\,mmHg = 0.1\,cmHg = \frac{(1.36\,g)(980\,cm/s^2)}{cm^2} = \frac{(1.36)(980)\,g}{cm \cdot s^2} \tag{19}$$

from which it follows that

$$1g = \frac{1}{(1.36)(980)(10)(60)^2}\,mmHg \cdot dm \cdot min^2 \tag{20}$$

Then, since the density of blood is approximately $1000g/dm^3$, we have the result that

$$\rho = 1000\frac{1}{(1.36)(980)(10)(60)^2} = 0.00002084167\,\frac{mmHg \cdot min^2}{dm^2} \tag{21}$$

Another complication in the use of equation (18) is that the shunt conductance G_{shunt} is flow-dependent. A simple idea here would be to use the shunt flow on the previous time step to set the shunt conductance for the present time step, but instead of this, we use fixed-point iteration, with the shunt flow on the previous time step as an initial guess. At each step of the fixed-point iteration, we use equation (18) to set the shunt conductance based on the latest guess for the shunt flow, we then write the shunt conductance into the appropriate two places in the conductance matrix G (one entry for each flow direction, since there is no valve involved in the shunt), and finally we solve for all of the pressures and flows of the circulation, including the shunt flow. We can see the benefit of doing the fixed-point iteration as it removes the numerical oscillations seen in the blood flow waveform in Figure 1. In practice, we use 10 fixed-point iteration steps in each time step, and this achieves good enough agreement between the flow that is used to set the shunt conductance and the flow that is calculated on the basis of that shunt conductance.
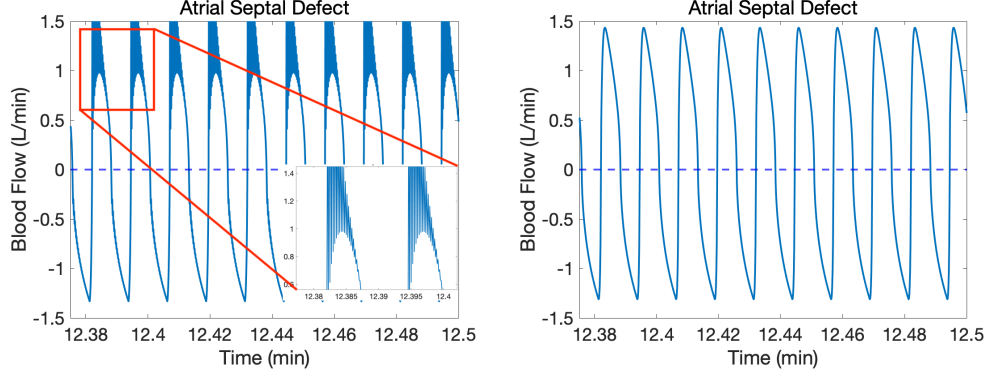
Figure 1: A comparison of results obtained without and with fixed-point iteration in ASD. The left panel shows flow computed without fixed-point iteration when the shunt area is $1cm^2$. The right panel shows flow computed with fixed-point iteration when the shunt area is $1cm^2$.

2.4 Oxygen transport model

An important consequence of the surgical interventions that we are considering is the mixing of oxygenated and doxygenated blood. Our approach to the modeling of oxygen transport follows [14]. Time-varying oxygen concentrations for each compliance chamber are described by the following system of differential equations:

$$\frac{d}{dt}([O_2]_i V_i) = \sum_{\substack{j=1 \\ j \neq i}}^{N} ([O_2]_j Q_{ji} - [O_2]_i Q_{ij} + M_{ji}), \tag{22}$$

where $[O_2]_i$ is the oxygen concentration in compliance chamber i, Q_{ji} is the blood flow from j to i, and M_{ji} is the rate at which oxygen is added to the stream of blood that is flowing from chamber j to chamber i. Note that M_{ji} is positive if oxygen is being added to the blood stream, and negative if oxygen is being removed. The correctness of equation (22) relies on the fact that all of the flows that appear in it are positive or zero. This is a benefit of our formulation in which every connection is equipped with a valve, as described above in section 2.1. These equations describe conservation of oxygen during transport between chambers as well as metabolic consumption of oxygen within systemic organs and replenishment of oxygen within the lungs. After computing the flows at timestep n, we use those computed flows to numerically update the oxygen concentrations from timestep $n-1$ to n as follows:

$$\frac{[O_2]_i^n V_i^n - [O_2]_i^{n-1} V_i^{n-1}}{\Delta t} = \sum_{\substack{j=1 \\ j \neq i}}^{N} ([O_2]_j^{n-1} Q_{ji}^n - [O_2]_i^{n-1} Q_{ij}^n + M_{ji}). \tag{23}$$

Note that this is the forward-Euler method insofar as the oxygen concentrations are concerned, although it differs from the forward-Euler method by using the flows at timestep n. The manner in which M is determined for use in these equations is described below.

We use the millimole ($mmol$) as the unit for the amount of oxygen. It then follows from our other choices of units that the units of oxygen concentration are $mmol/L$ and the units of the rate of oxygen consumption by the body are $mmol/min$. A standard concentration of hemoglobin in blood is 2.5 $mmol/L$, and since each hemoglobin molecule can carry four oxygen molecules, the oxygen concentration when hemoglobin is fully saturated is 10 $mmol/L$.

8

There are only two places in our model where the variable M that appears in equation (22) is nonzero. One of these is in the connection from the pulmonary arteries (pa) to the pulmonary veins (pv). We assume that $M_{pa,pv}$ is such that the stream of blood flowing from the pulmonary arteries to the pulmonary veins becomes fully saturated with oxygen during its passage through the pulmonary capillaries. This gives the equation

$$M_{pa,pv} = (10 \; mmol/L - [O_2]_{pa})Q_{pa,pv}. \tag{24}$$

We use this equation (24) to set $M_{pa,pv}$ at every time step. Note that this is *not* the same as setting $[O_2]_{pv} = 10 \; mmol/L$. The reason is that there may be other streams of blood entering the pulmonary venous compartment besides the one coming from the pulmonary arteries. In particular, since we regard the left atrium as being part of the pulmonary venous compartment, this will be the case when we are simulating a surgically created atrial septal defect.

The other nonzero value of M in our model is $M_{sa,sv}$, which is negative, since it represents oxygen consumption by the tissues. This oxygen is extracted from the stream of blood that flows from the systemic arteries (sa) to the systemic veins (sv). In the simulations reported here, we keep $M_{sa,sv}$ constant, and we choose its value by noting that a normal cardiac output is 5.6 L/min and a normal amount of oxygen extraction by the systemic tissue is 30%. This gives the following:

$$-M_{sa,sv} = 0.3 \cdot (10 \; mmol/L) \cdot (5.6 \; L/min) = 16.8 \; mmol/min \tag{25}$$

As an initial condition, we set the oxygen concentration equal to 10 $mmol/L$ in all compartments, and then we run the simulation until all hemodynamic variables and oxygen concentrations have reached a periodic steady state. The values we report are averages over the last 10 of the computed cardiac cycles.

3 Results and Discussion

In this section, we examine the simulated consequences of each of the three interventions in which pulmonary hypertension is intended to be alleviated by creating a shunt in the form of an ASD, VSD, or PDA. We first investigate changes in pressure and oxygen saturation in the systemic and pulmonary arteries as the shunt size is varied. Second, we examine the direction of shunt flow to determine whether the shunt is indeed right-to-left as intended or perhaps bidirectional. In the simulations reported here, we use 100 time steps for each cardiac cycle. The heart rate is 80 beats/minute, and we run each computer experiment for 12.5 minutes of simulated time, thus covering 1,000 simulated heartbeats. This duration is sufficient for the simulation to achieve a periodic steady state for all variables in all cases. When we report a single value for any quantity as the result of simulation, it is the average of that quantity over the last 10 cardiac cycles of the simulation.

3.1 Pressures and oxygen saturations

First, we consider the blood pressures and oxygen saturations for each intervention. Figure 2 shows the systemic and pulmonary arterial blood pressures (mean values) as functions of shunt area. Results for the atrial septal defect (ASD) are in the left panel, results for the ventricular septal defect (VSD) are in the middle panel, and results for the patent ductus arteriosus (PDA) are in the right panel. The ASD result shows that this intervention is not successful in lowering the pulmonary

arterial pressure. (The insets in the figure shows that there is a very small effect, but it is certainly not one that would be therapeutic.) The simulated VSD intervention lowers the mean pulmonary artery pressure from about 105 $mmHg$ to about 85 $mmHg$, which could be beneficial. This result is achieved by a shunt with the cross-sectional area 0.6 cm^2, and it is interesting that beyond this point the pulmonary arterial pressure increases slightly as the shunt size increases. The PDA result produces the best lowering of the mean pulmonary arterial blood pressure, from about 105 $mmHg$ to about 75 $mmHg$. Unlike in the VSD case, the pulmonary arterial mean blood pressure with a PDA decreases monotonically with increasing shunt size, but most of the benefit has already occurred with a shunt size of 0.5 $mmHg$, so there is a little benefit to using a larger PDA than this. Figure 3 shows the pressures in pulmonary artery and systemic artery for three interventions, all on the same plot, as functions of shunt area.
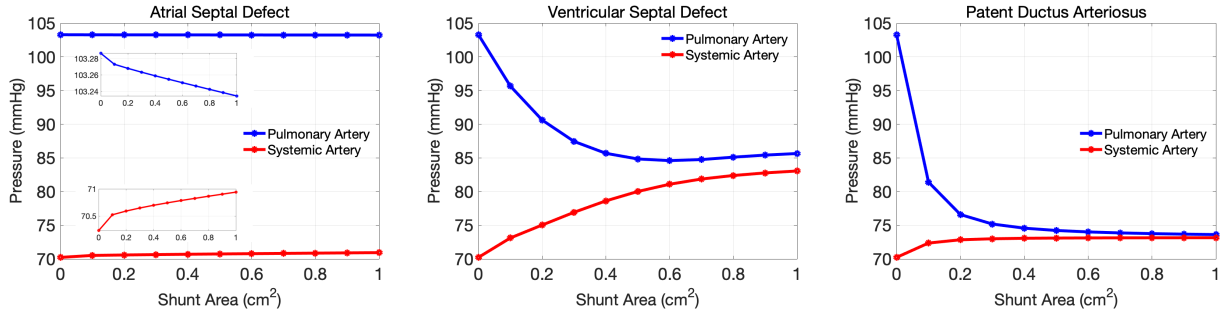

Figure 2: A comparison of pressures in the pulmonary artery (blue) and systemic artery (red) as the shunt area is varied in the ASD, VSD, and PDA. The inset figure shows a zoomed in portion of the results.
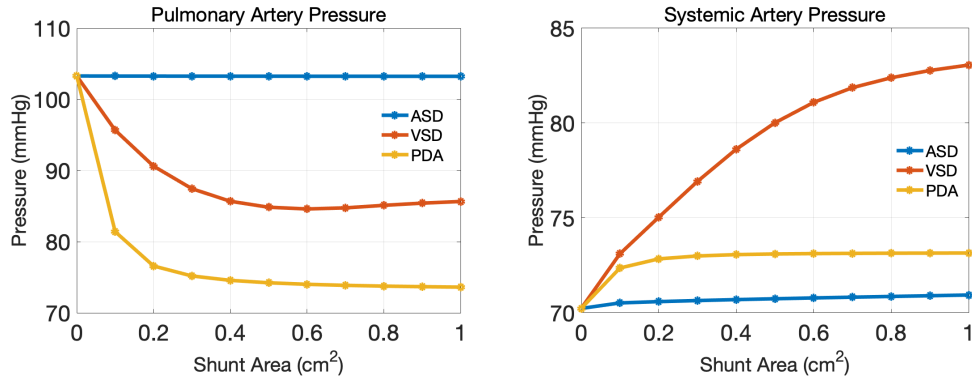

Figure 3: A comparison of pressures in pulmonary artery and systemic artery for the three interventions: the left panel shows the pulmonary artery pressures for the three interventions as the shunt area is varied. The right panel shows the systemic artery pressures for the three interventions as the shunt area is varied. Note different pressure scales in the two panels.

We further investigate oxygen transport for each intervention in Figure 4. All three interventions increase systemic flow. The increase is substantial, however, only in the case of VSD, where the increase in systemic flow has a substantial effect on oxygen delivery to the systemic tissues, as discussed below. All three interventions decrease systemic arterial oxygen saturation. This is inevitable, since the intervention by design are allowing venous blood to bypass the lungs. The effect is smallest in the case of ASD, but since the ASD intervention had essentially no benefit,

the fact that it also does the least harm is not really of interest. The VSD and PDA interventions produce similar decreases in systemic arterial oxygen saturation, but these two interventions look quite different from the point of view of oxygen delivery to the systemic tissues. Here the increase in systemic flow in the VSD case seems to compensate nicely for the drop in systemic arterial oxygen saturation. Even at the shunt size of 0.4 cm^2, where the oxygen delivery is the smallest in the VSD case, it is only about 4% smaller than in the pre-intervention state with zero as the shunt size. Recall, however, that the optimal reduction in pulmonary arterial blood pressure occurs in the case of VSD at a shunt size of 0.6 cm^2, and at this shunt size, the reduction of oxygen delivery is even smaller – only about 2.5%.
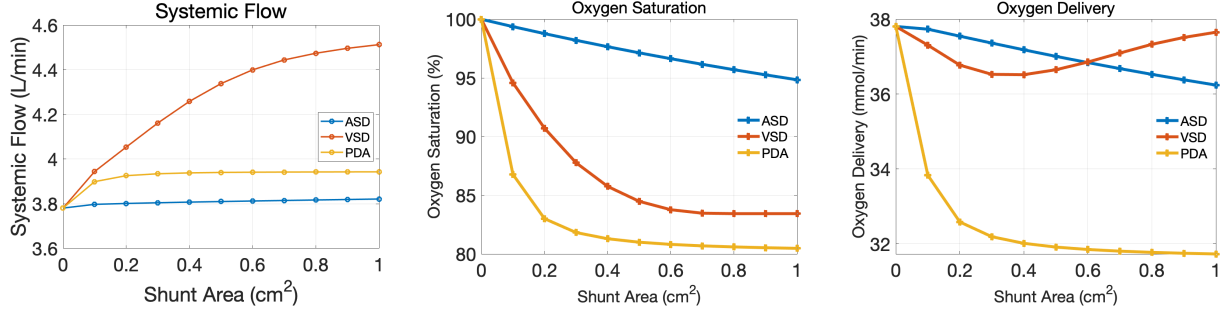

Figure 4: A comparison of systemic flow, oxygen saturation, and oxygen delivery rate for the three interventions: the left panel shows the systemic flow, the middle panel shows the oxygen saturation, and the right panel shows the rate of oxygen delivery to the systemic tissues.

Figure 4 shows systemic flow, oxygen saturation, and the rate of oxygen delivery for three interventions. Systemic flow is relevant here because it is used in the computation of oxygen delivery to the systemic tissues. Oxygen saturation is the oxygen concentration (in $mmol/L$) expressed as a percentage of 10 $mmol/L$. It is the maximum possible oxygen concentration in our model. The rate at which oxygen is delivered to the systemic tissues is calculated by multiplying the systemic flow by the systemic arterial oxygen concentration.

3.2 Shunt flow waveforms

Figures 5, 6, and 7 show waveforms of the shunt flow in each of the three interventions, ASD, PDA, and VSD, for two particular shunt sizes, 0.1 cm^2 and 1 cm^2. The last 10 cardiac cycles of a 1000-cycle computer simulation are shown in each case. In all cases, our sign convention is that right-to-left flow is considered positive. Note that the ASD shunt flow is strongly bidirectional, whereas the VSD and PDA flows are exclusively right-to-left. The VSD flow is essentially zero, however, during part of each cardiac cycle, whereas the PDA flow never comes close to zero, but instead is sustained right-to-left flow throughout the cardiac cycle.

Although bidirectional flow does not play an important role in this study, since the ASD intervention does not appear to be useful, it is an important feature of our methodology that it evaluates the shunt flow as a function of time, and not merely the mean flow. This is because bidirectional flow can exchange oxygen between two compartments even when there is no mean shunt flow at all, and this can have a substantial impact on oxygen transport. Indeed, in the congenital heart disease transposition of the great arteries, the pulmonary and systemic circulations form parallel loops, and there cannot be any mean flow from one to the other. Survival of the patient after birth is then completely dependent on the existence of a bidirectional shunt [14].
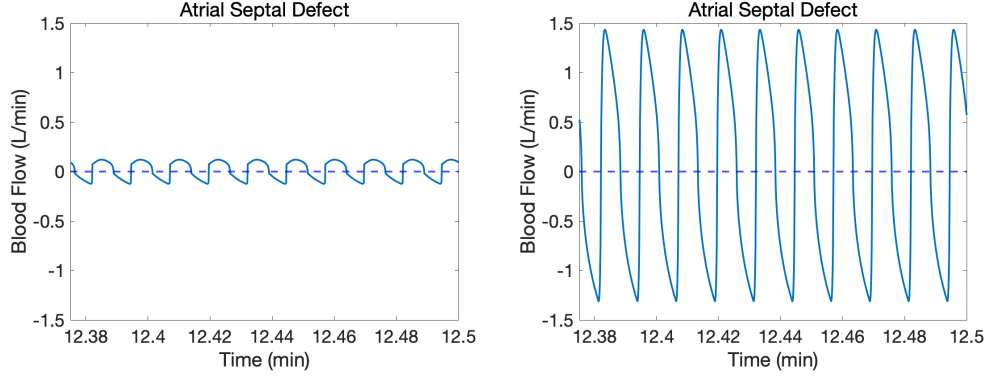
Figure 5: Shunt flow waveforms in the ASD. The left panel shows flow when the shunt area is 0.1 cm^2, and the right panel flow when the shunt area is 1 cm^2.
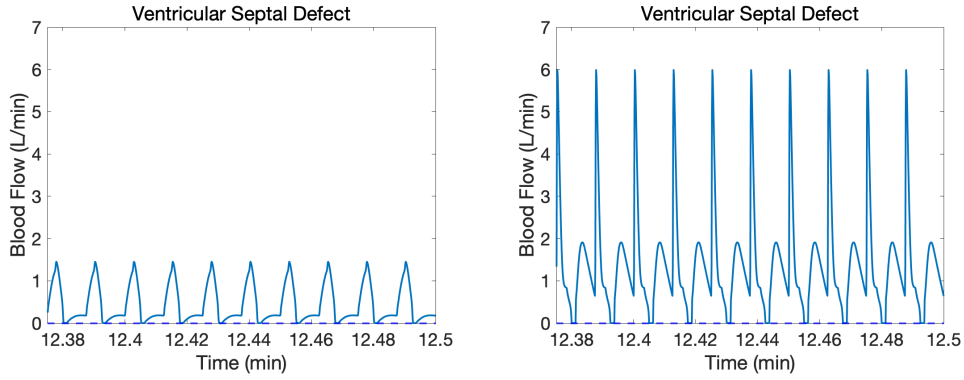

Figure 6: Shunt flow waveforms in the VSD. The left panel shows flow when the shunt area is 0.1 cm^2, and the right panel flow when the shunt area is 1 cm^2.
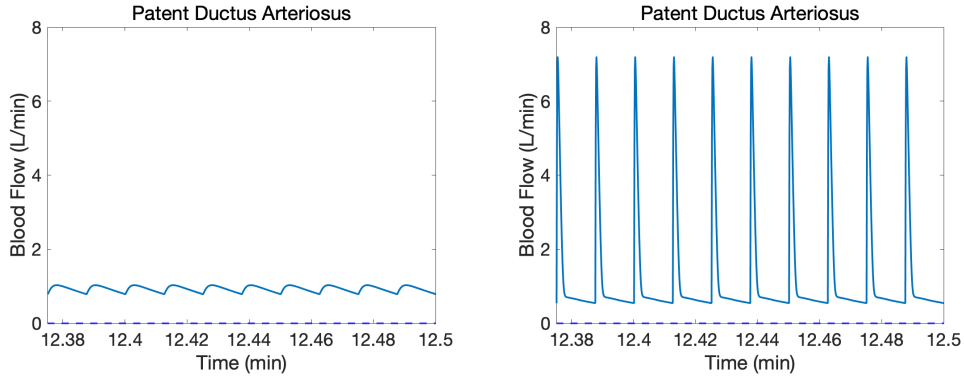

Figure 7: Shunt flow waveforms in the PDA. The left panel shows flow when the shunt area is 0.1 cm^2, and the right panel shows flow when the shunt area is 1 cm^2.

4 Conclusions

In this paper, we have presented a methodology that can be used to predict the effects of surgical interventions designed to alleviate refractory pulmonary hypertension. We have illustrated the use of this methodology by comparing three such interventions, all of which are designed to allow some

blood flow to bypass the lungs. We have named these interventions by the congenital heart disease that they effectively create: atrial septal defect (ASD), ventricular septal defect (VSD), and patent ductus arteriosus (PDA). For each intervention, we have simulated a range of defect sizes from 0 to 1 cm^2. Our results are that ASD is ineffective at lowering the blood pressure in the pulmonary artery, but that VSD and PDA are both effective, with the greater effect being produced by the PDA intervention. Both VSD and PDA lower the systemic arterial oxygen saturation in our study, but this is partially compensated by an increase in systemic flow, so that oxygen delivery to the systemic tissues is lowered to a lesser degree than the systemic arterial oxygen saturation. The increase in systemic flow is substantially greater for VSD than for PDA, with the result that oxygen delivery is only slightly reduced in the VSD case, but more substantially reduced in the case of PDA. Thus, when judged by reduction of pulmonary arterial pressure alone, PDA appears to be the best choice in our study, but when oxygen delivery is also considered the choice between PDA and VSD is less clear. All of the above effects are quantified in our study as functions of the size of the defect in each case, and this kind of information could be useful to a surgeon who needs to decide how large a defect to create.

These specific conclusions are intended, however, only to illustrate what our methodology can do, and should not be applied to any particular patient. The reason for this is that the results of our study may depend very much on the particular parameters used, and we have only considered one particular parameter set here. In order to apply the methodology of this paper with confidence to any particular patient, it would be necessary to identify the relevant cardiovascular parameters of that patient, so that the model can be made patient-specific. How to do this is a research problem in itself, and one that we intend to tackle in future work.

Aside from the issue of parameters, there is also the possibility that the model itself will need improvement before it can be deemed realistic enough for practical use. All models are idealized, and the question of how limiting those idealizations are can only be settled by comparison to real-world observations. In this case, studies are needed in which model results are compared to the surgical outcomes of patients with refractory pulmonary hypertension who have actually undergone one of the interventions that we have considered in this paper.

Even though the detailed conclusions of this paper may change as a result of further research, either because of changes in parameters, or because of more fundamental changes in the model itself, we hope that the results presented here can at least serve the purpose of illustrating how mathematical modeling might prove useful as an aid to the surgical decision-making process.

References

[1] Sebastián Acosta, Charles Puelz, Béatrice Rivière, Daniel J Penny, Ken M Brady, and Craig G Rusin. Cardiovascular mechanics in the early stages of pulmonary hypertension: a computational study. *Biomechanics and Modeling in Mechanobiology*, 16(6):2093–2112, 2017.

[2] Alban-Elouen Baruteau, Emre Belli, Younes Boudjemline, Daniela Laux, Marilyne Lévy, Gérald Simonneau, Adriano Carotti, Marc Humbert, and Damien Bonnet. Palliative potts shunt for the treatment of children with drug-refractory pulmonary arterial hypertension: updated data from the first 24 patients. *European Journal of Cardio-Thoracic Surgery*, 47(3):e105–e110, 2015.

[3] Tammo Delhaas, Yvette Koeken, Heiner Latus, Christian Apitz, and Dietmar Schranz. Potts shunt to be preferred above atrial septostomy in pediatric pulmonary arterial hypertension patients: a modeling study. *Frontiers in Physiology*, 9:1252, 2018.

[4] Christian D Etz, Henryk A Welp, Tony DT Tjan, Andreas Hoffmeier, Ernst Weigang, Hans H Scheld, and Christof Schmid. Medically refractory pulmonary hypertension: treatment with nonpulsatile left ventricular assist devices. *The Annals of Thoracic Surgery*, 83(5):1697–1705, 2007.

[5] Frank C Hoppensteadt and Charles S Peskin. *Modeling and simulation in medicine and the life sciences*, volume 10. Springer Science & Business Media, 2012.

[6] Jane A Leopold. Catheter-based therapies for patients with medication-refractory pulmonary arterial hypertension. *Circulation: Cardiovascular Interventions*, 8(11):e003332, 2015.

[7] Marilyne Levy, David S Celermajer, Elisabeth Bourges-Petit, Maria-Jesus Del Cerro, Fanny Bajolle, and Damien Bonnet. Add-on therapy with subcutaneous treprostinil for refractory pediatric pulmonary hypertension. *The Journal of Pediatrics*, 158(4):584–588, 2011.

[8] Fuyou Liang, Shu Takagi, Ryutaro Himeno, and Hao Liu. Multi-scale modeling of the human cardiovascular system with applications to aortic valvular and arterial stenoses. *Medical & biological engineering & computing*, 47(7):743–755, 2009.

[9] JP Mynard, MR Davidson, DJ Penny, and JJ Smolich. A simple, versatile valve model for use in lumped parameter and one-dimensional cardiovascular models. *International Journal for Numerical Methods in Biomedical Engineering*, 28(6-7):626–641, 2012.

[10] Charles S Peskin and Cheng Tu. Hemodynamics in congenital heart disease. *Computers in biology and medicine*, 16(5):331–359, 1986.

[11] M Umar Qureshi, Gareth DA Vaughan, Christopher Sainsbury, Martin Johnson, Charles S Peskin, Mette S Olufsen, and NA Hill. Numerical simulation of blood flow and pressure drop in the pulmonary arterial and venous circulation. *Biomechanics and Modeling in Mechanobiology*, 13(5):1137–1154, 2014.

[12] Terry Reynolds. The determination of aortic valve area by the gorlin formula: what the cardiac sonographer should know. *Journal of the American Society of Echocardiography*, 3(4):331–335, 1990.

[13] Nikos Stergiopulos, Jean-Jacques Meister, and Nico Westerhof. Determinants of stroke volume and systolic and diastolic aortic pressure. *American Journal of Physiology-Heart and Circulatory Physiology*, 270(6):H2050–H2059, 1996.

[14] Cheng Tu and Charles S Peskin. Hemodynamics in transposition of the great arteries with comparison to ventricular septal defect. *Computers in biology and medicine*, 19(2):95–128, 1989.